

A Planar Interdigital Sensor for Bio-impedance Measurement: Theoretical analysis, Optimization and Simulation

Thanh-Tuan Ngo ^{*}, Hamidreza Shirzadfar [†], Djilali Kourtiche, Mustapha Nadi

Université de Lorraine-CNRS, UMR 7198, Institut Jean Lamour, Vandœuvre-lès-Nancy, France

(Received 28 January 2014; published online 06 April 2014)

This paper proposes the design of a biosensor to characterize the dielectric and conductive properties of biological materials (for example blood or water) by impedance spectroscopy. Particularly, its design optimized the geometric structure interdigitated electrodes. This optimization allows extending the frequency range of measurement by reducing the polarization effect. Polarization effect is manifested by an interface capability (or double layer) from interaction between ions and molecules in the boundary between the surface of the electrolyte and the electrodes, it increases the measurement error at low frequencies. This paper recommends also a novel method to determine the parameters (relative permittivity, thickness and capacitance per unit area) of the double layer (DL) at the contact surface of the electrode with the solution. CoventorWare software was utilized to modelize of interdigital sensor structure in three dimensions (3D) to verify the analytical results and evaluate the influence of geometrical parameters and the dielectric properties of the medium on bioelectrical impedance.

Keywords: Interdigitated sensor, Optimization, Impedance spectroscopy, Double layer, Biological medium.

PACS numbers: 87.85.fk, 85.85. + j

1. INTRODUCTION

The characterization of biological mediums can benefit from the impedance spectroscopy. Dielectric and conductive properties of biological as well as their frequency dependence due to the phenomena of relaxations mediums encourage this type of approach. Constraints related to low frequency measurements are also a challenge for the dielectric characterization of biological medium. Polarization phenomena well known impedance spectroscopy become very restrictive for applications at the cellular level.

The geometry of a sensor is optimized for bio-impedance measurements may induce an increase of the measuring range and a decrease in errors. Pejčić et al [1] pointed out that the optimization of the design of the electrodes of a sensor is one of the most crucial steps in the realization of a bio impedance measurement device. Pejčić's experiments were performed to optimize electrode designs for various applications. R. Igreja et al [2] have represented new analytical expressions for the capacitance between the two comb electrodes of a periodic interdigital capacitive sensor, based on conformal mapping techniques. The effect of the interdigitated electrode geometry (electrode width and spacing) and electro ceramic substrate thickness on the developed strain for bulk PZT substrates was modeled by C. Bowen et al [3]. They have described in detail the optimisation of interdigitated electrodes for piezoelectric actuators and active fibre composites. F.Alexander et al [4] have optimized a interdigital sensor for impedance based evaluation of HS 578T cancer cells. Wang et al [5] have determined the sensitivity and frequency characteristics of coplanar electrical cell-substrate impedance sensors. All these microelectrode optimizations were made for specific applications. The optimization studies which mentioned were made based on

arbitrary changes of the geometric parameters. The volume of sample in contact with the electrodes is not similar in each assay, and therefore unsuitable optimizations.

Additionally, Ibrahim et al [6, 7] have optimized a sensor microelectrodes and similar in each assay, but in their work was missed the optimization the length of electrodes.

This paper presents a new approach of physical and electrical modeling system of a biological sensor. We propose a theoretical optimization of the geometrical parameters of the sensor by developing total impedance equations and modeling equivalent circuits. Furthermore, this work demonstrates a theoretical calculation to determine the relative permittivity, thickness and capacitance parameters of the double layer in the contact the electrodes with solutions. The electrical and physical models of an interdigital sensor were designed by using CoventorWare software. In following, we have studied the influence of the medium's physical properties on the frequency sensor response. Moreover, this research also describes the correlation between the design parameters and the frequency behavior in coplanar impedance sensors.

2. THEORETICAL ANALYSIS AND OPTIMIZATION

2.1 Equivalent Circuit Model

An interdigital sensor is formed of two metal electrodes comb-shaped, each electrode has a width W , a length of electrodes L and a distance between two consecutive electrodes S [8, 9, 10] (see Fig. 1). This sensor is deposited on a thin glass substrate. When an electric voltage U between the two electrodes is applied, this voltage creates an electric field between each pair of electrodes.

^{*} thanh-tuan.ngo@univ-lorraine.fr

[†] hamidreza.shirzadfar@univ-lorraine.fr

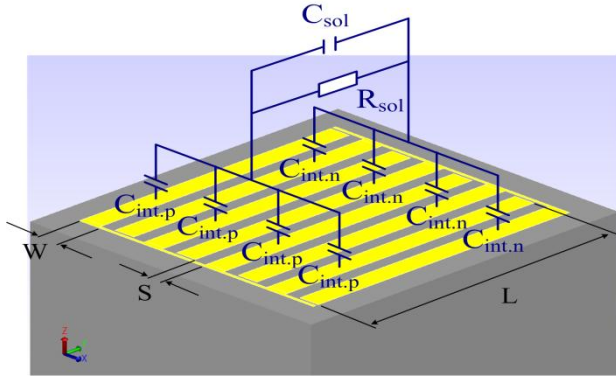


Fig. 1 – Schema of the equivalent circuit model. C_{sol} and R_{sol} present the dielectric properties of the medium under testing, and $C_{int.p}$, $C_{int.n}$ indicate the properties of the double layer phenomena at the contact surface of each electrode

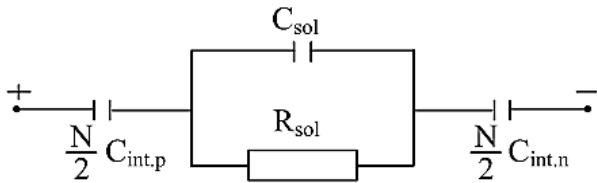


Fig. 2 – Simplified equivalent circuit model of interdigitated sensor

Fig. 1 shows the schematic of the sensor's equivalent circuit model, the structure of the sensor (8 interdigitated electrodes) and its geometrical parameters. The simplified equivalent circuit is adopted when such a cell is immersed in an electrolyte solution and is shown in Fig. 2.

The different ingredients of biological impedance Z (which is measured by sensor) is described by the electrical components (C_{sol} and R_{sol}). Where R_{sol} represents the conductive properties of the solution under the effect of an electric field; and it is also called the resistance of the electrolyte solution. This component is the sensitive measuring element. According to Olthuis [11, 12] R_{sol} is related to the conductivity of the medium σ and the cell factor K_{cell} , and the cell factor K_{cell} depends entirely on the geometry of the sensor.

$$R_{sol} = \frac{K_{cell}}{\sigma} \quad (2.1)$$

$$K_{cell} = \frac{2}{L(N-1)} \cdot \frac{K(k)}{K(\sqrt{1-k^2})} \quad (2.2)$$

where $k = \cos\left(\frac{\pi}{2} \cdot \frac{W}{S+W}\right) = \cos\left(\frac{\pi \cdot a}{2}\right)$; with

$a = \frac{W}{S+W}$ is the metallization ratio (for example: $a = 0.4$ means 40 % of metallization). This parameter has great relevance with the cut-off frequency $f_{cut-off}$, as will be shown in the next part (optimization of the metallization ratio). The function $K(k)$ is the incomplete elliptic integral of the first module k is cell factor (m^{-1}); σ is electrical conductivity (S/m); N is number of electrodes.

The capacitance C_{sol} represents the capacitance of

the solution to be measured. The capacitance $C_{int.p}$ represents the capacitance at the contact surface of each positive electrode with the solution to be measured and the capacitance $C_{int.n}$ represents the capacitance at the contact surface of a negative electrode with the solution to be measured. They are determined by:

$$C_{int.p} = C_{int.n} = LWC_0 \quad (2.3)$$

where C_0 is the capacitance per unit area ($pF / \mu m^2$).

For the reason that the number of negative electrode and number of positive electrode are the same ($N/2$), therefore the equivalent capacitance at the negative electrode and at the positive electrode is determined by:

$$\frac{N}{2} C_{int.p} = \frac{N}{2} C_{int.n}$$

Consequently, the total capacitance at the contact surface is determined by:

$$C_{interface} = \frac{N}{4} \cdot LWC_0 \quad (2.4)$$

By definition the electrical impedance quantifies the behavior of a medium interacting with a field or current. The impedance Z reflects the correlation between the voltage at the terminals of a circuit and the current through the sample. In a homogeneous and isotropic medium linear material, the impedance is not a function of its electrical properties such as conductivity σ and permittivity ϵ , but also depends on the geometric factors of the cell [13, 14, 15] and it is described by expression:

$$Z = \frac{K_{cell}}{\sigma + j\omega\epsilon_0\epsilon_r} \Rightarrow Y = G + j\omega C = \frac{\sigma + j\omega\epsilon_0\epsilon_r}{K_{cell}} \Rightarrow \begin{cases} G = \frac{\sigma}{K_{cell}} \\ C = \frac{\epsilon_0\epsilon_r}{K_{cell}} \end{cases} \quad (2.5)$$

where j is imaginary symbol; ω is angular pulsation (rad / s); ϵ_0 is permittivity of vacuum: 8.8542×10^{-12} (F / m); ϵ_r is relative permittivity of the medium; Z is complex impedance (Ω); Y is complex admittance (S); G is susceptance (S); C is capacitance (F).

On the other hand, according to the equivalent electric circuit (see Fig. 2) the total impedance can be determined by:

$$\begin{cases} Z = \frac{1}{G_{sol} + j\omega C_{sol}} + \frac{1}{j\omega C_{interface}} \\ Y = \frac{1}{Z} = G + j\omega C \end{cases} \quad (2.6)$$

After shortened the equation (2.6), we can calculate the conductance G and the capacitance C .

$$\Rightarrow \begin{cases} G = \frac{\omega^2 G_{sol} C_{interface}^2}{G_{sol}^2 + \omega^2 (C_{sol} + C_{interface})^2} \\ C = \frac{C_{interface} G_{sol}^2 + \omega^2 C_{sol} C_{interface} (C_{sol} + C_{interface})}{G_{sol}^2 + \omega^2 (C_{sol} + C_{interface})^2} \end{cases} \quad (2.7)$$

2.2 Optimization of the Metallization Ratio

The main objective of this work is the geometric optimization of the sensor structure to extend the range of cut-off frequency measurement. The cut-off frequency is equal to interface impedance of solution and is given by:

$$f_{cut-off} = \frac{1}{2\pi \cdot R_{sol} C_{interface}} \quad (2.8)$$

In this research, we use a square structure of $L \times L$ (the total width and the long of electrodes are the same). For an electrode structure with a pair of interdigitated electrodes number, the total width of the structure is given by: $L = N(W + S) - S$. Because of the dimension of L is more bigger than S , we can make the following approximation [7]:

$$L \approx N \cdot (W + S) \Rightarrow N = \frac{L}{W + S} \quad (2.9)$$

In the replacing R_{sol} from equation (2.1), K_{cell} from (2.2), $C_{interface}$ from (2.4) and N from (2.9), the equation of cut-off frequency (2.8) can be rewritten as:

$$f_{cut-low} = \frac{\sigma}{\pi \cdot C_0} \cdot \frac{N-1}{L \cdot a} \cdot \frac{K(\sqrt{1-k^2})}{K(k)} \quad (2.10)$$

Fig. 3 presents the relative between the cut-off frequency and the metallization ratio a . The simulation parameters are as follows $\sigma = 0,7 \times 10^6 (pS / \mu m)$; $C_0 = 4,5 \times 10^{-3} (pF / \mu m^2)$; $N = 50$; $L = 2mm$.

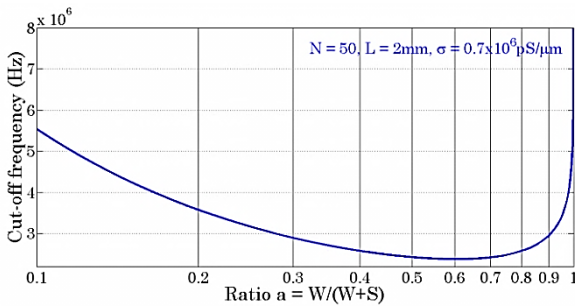


Fig. 3 – The cut-off frequency of sensor with 50 electrodes as a function of the metallization ratio a

As observe from Fig. 3, the minimum part of cut-off frequency happens in $a = 0.6$.

Fig. 4 demonstrates the cut-off frequency of several interdigitated electrodes as a function of the metallization ratio. The simulation results are obtained by following parameters:

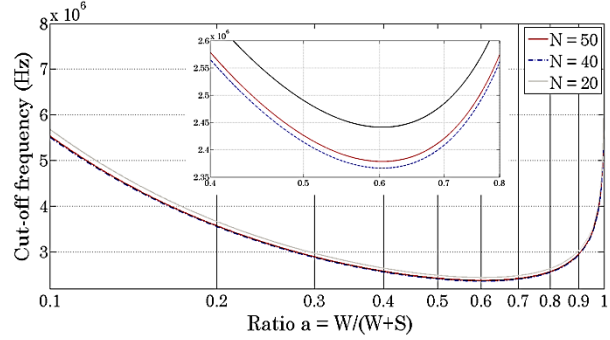


Fig. 4 – The cut-off frequency of three different sensor electrodes ($N = 20, 40, 50$) as a function of the metallization ratio a

- $N = 50; L = 2mm; C_0 = 4.5 \times 10^{-3} (pF / \mu m^2)$
- $N = 40; L = 2mm; C_0 = 3.6 \times 10^{-3} (pF / \mu m^2)$
- $N = 20; L = 2mm; C_0 = 1.7 \times 10^{-3} (pF / \mu m^2)$

Furthermore, Fig. 4 justifies that the minimum cut-off frequency in whole constructions correspond to a value of $a = 0.6$. According to the theoretical results, we will choose the metallization ratio: $a = W / (S + W) = 0.6$ to optimize the structure of sensor interdigitated electrodes.

2.3 Optimization the Length of Electrodes L

Fig. 5 shows the cut-off frequency as a function of the length of electrodes L from formula (10). The parameters of this simulation corresponding with the number of electrode which equal to $N = 50$ and the value of the metallization ratio ($a = 0.6$).

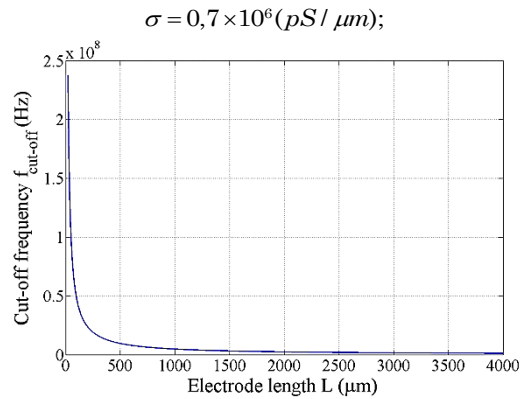


Fig. 5 – The theoretical result of cut-off frequency as a function of the length of electrodes L for optimization of $a = 0.6$

Fig. 6 indicates the comparison between the cut-off frequency for different number of electrodes ($N = 20$; $N = 40$; $N = 50$) and the length of electrodes (L). From Fig. 5 and Fig. 6, we can realize that variation of cut-off frequency was strongly decreased when $L < 2000 \mu m$; and when $L > 2000 \mu m$ the cut-off frequency variations are almost negligible.

As mentioned before, when measuring on biological samples of micrometric dimensions, it is preferable to use electrode structures which have the lowest impedance module R_{sol} . The contact surface of interdigital sensor is more bigger than the surface of the sensor with 2 or 4

electrodes which presented in [16], for this reason the interface capacities is much greater and the influence of polarization effect is more smaller (see Appendix).

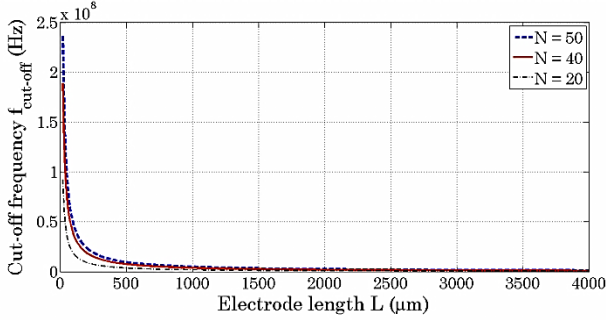


Fig. 6 – The theoretical results of cut-off frequency for different electrodes (N) as a function of the length of electrodes L for optimization of $\alpha = 0.6$

We examined the influence of the length of electrodes L on the cell factor K_{cell} (see Fig. 7); additionally, the influence of electrode number N on the cell factor K_{cell} is calculated and indicated in Fig. 8.

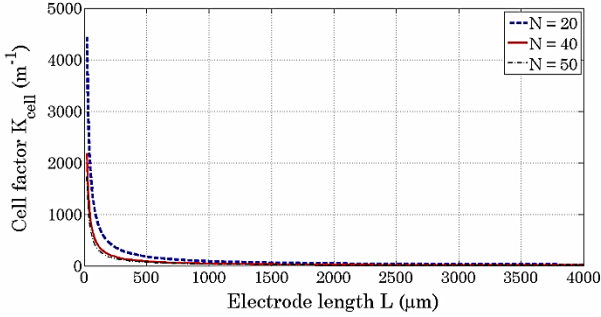


Fig. 7 – The theoretical result of cell factor K_{cell} as a function of the length of electrodes L for optimization of $\alpha = 0.6$

Fig. 7 presents the behavior between the cell factor (K_{cell}) and the length of electrodes (L) in various type of electrodes ($N = 20$; $N = 40$; $N = 50$). We can point out from Fig. 7 that the cell factor K_{cell} decreases with the length of electrodes. We can also observe a wide variation of cell factor in condition $L < 2000 \mu\text{m}$, therefore when $L > 2000 \mu\text{m}$, the change of K_{cell} is insignificant.

Hence, from Fig. 5, Fig. 6 and Fig. 7, we can select $L = 2000 \mu\text{m}$ as a theoretical optimization of interdigitated electrodes.

2.4 Optimization of the Electrode Number N

The optimal number of electrodes can be minimum equal to $N=2$ which is the lowest possible number of electrodes. Moreover, the sensitivity of the impedance measurement depends on the number of electrodes. Thus, the modeling allows us to study the influence of the number of electrodes in the impedance measurement.

Fig. 8 shows the theoretical results of the cell factor K_{cell} as a function of the electrode number N from formula (10) for different length of electrodes ($L = 1 \text{ mm}$, $L = 2 \text{ mm}$, $L = 3 \text{ mm}$). In Fig. 8, we find a decrease of the cell factor with increase the number of electrode. We observe a large variation in the cell factor of N in the range from 2 until 40 electrodes. In following, the variations

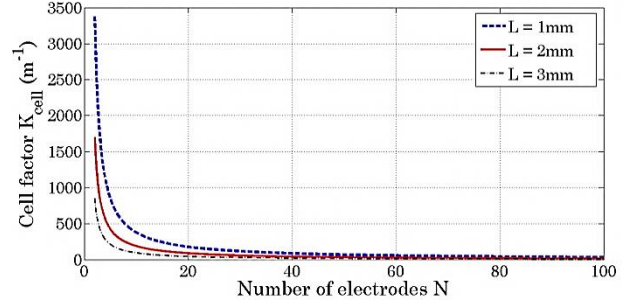


Fig. 8 – The various sensor cell factors K_{cell} with electrode length ($L = 1 \text{ mm}$, $L = 2 \text{ mm}$, $L = 3 \text{ mm}$) as a function of N with ratio $\alpha = 0.6$

in the cell factor are very weak for $N > 40$. For this purpose, we can choose $N = 40$ as a theoretical optimization of interdigitated electrodes.

3. MODELIZATION OF INTERDIGITATED SENSOR BY COVENTORWARE SOFTWARE

We have used the simulation software (CoventorWare) program to verify the theoretical results which achieved in previous part. This simulation permits to evaluate the influence of geometrical parameters of the interdigitated structure of the sensor and the dielectric properties of the medium on bioelectrical impedance (see Fig. 9). In this section, we describe the design of the physical model of the sensor loaded by a biological medium (for example blood). We have utilized the module MEMS electroquasistatic harmonic response which is proposed by this software. It should be remarked that in this structure the medium must place in a homogeneous and isotropic medium liner materials.

3.1 Modelization of Sensor's Electrodes

In this simulation is created the micrometer scale interdigital sensor structure to measure the impedance of samples. This sensor consists of two superimposed layers, the first layer forms as a glass substrate and the second layer arrangements like a structure of the platinum electrodes. The 3D view of sensor is given in Fig. 9. The first layer consists of a square shape with dimension of $2600 \mu\text{m}$ and with a thickness of $1000 \mu\text{m}$. Due to the glass substrate which is a good electrical insulator; we do not need to put an insulating layer between the electrodes and the substrate. Furthermore, platinum is one of the best conductor to produce the electrodes of interdigital sensor, platinum's conductivity is equal to $9.42 \times 10^6 \text{ Sm}^{-1}$.

In the simulation program, we have selected platinum mask (cover) electrodes with a thickness $1 \mu\text{m}$ and were deposited on the substrate (layer 2). The total area occupied by the electrodes corresponds to that of a square of side $L = 2000 \mu\text{m}$.

3.2 Modelization of the Medium

As shown in Fig. 1, the components $C_{int,p}$, $C_{int,n}$, C_{sol} and R_{sol} present the electrical properties of the medium. The two components $C_{int,p}$, $C_{int,n}$ describe the phenomena of polarization at the boundary between the surface of the electrolyte and the electrodes. Moreover,

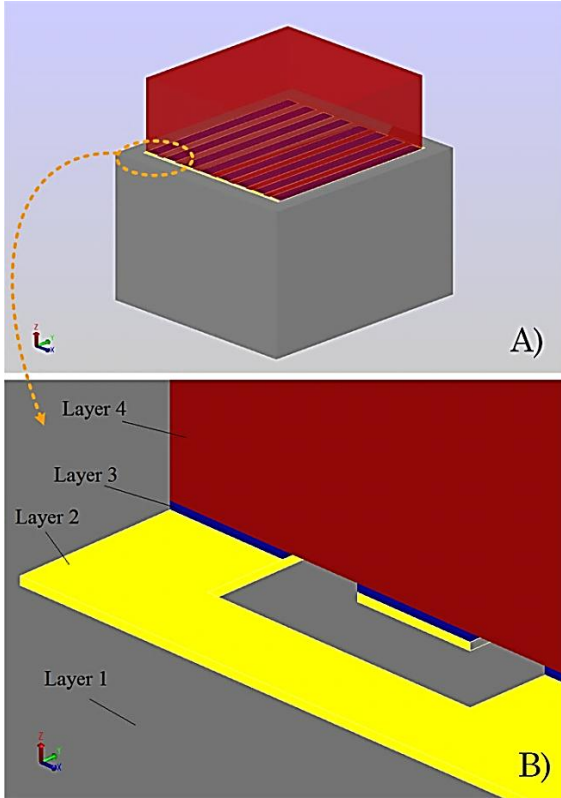


Fig.9 – The 3D view model of 16 electrodes type planar interdigitated electrode loaded by the full medium, which contains the double layer DL and blood medium. First layer of system is deposited by a glass substrate (A). Second layer consists of interdigitated electrodes, third layer presents the phenomena and properties of the double layer and fourth layer describes the dielectric properties of the blood medium (B)

we will need two layers to represent the medium’s electrical properties and interface polarization. Thus, the total medium of model consists of two layers as shown in Fig. 9. Layer 3 represents the properties of interface polarization electric properties ($C_{interface}$) and layer 4 describes the electrical properties of medium R_{sol} , C_{sol} with a thickness of 500 μm . We have verified the model of blood as a biological medium with the conductivity $\sigma=0.7 \text{ S/m}$ in the frequency range 10 Hz-1 GHz. The determination of the parameters at the layer 3 (relative permittivity, thickness) are very important to simulate the sensor.

From formula (2.7), at low frequency the ω is approximately equal to zero and the value of total capacity (C) may be calculated by the following equation:

$$\lim_{\omega \rightarrow 0} C = C_{interface} \quad (3.1)$$

By replacing C from equation (2.5) and $C_{interface}$ from formula (2.4), the equation (3.1) becomes:

Table 1 – The simulation parameters of the interdigital sensor

Sensor	L (mm)	N	W (μm)	S (μm)	a	K_{cell} (m^{-1})	C_0 ($\text{pF} / \mu\text{m}^2$)	$\epsilon_{r,DL}$	d_{DL} (μm)
1	2	40	15	35	0.3	35.8	4.37×10^{-3}	493.5	1
2	2	40	30	20	0.6	21.8	3.6×10^{-3}	405	1
3	2	40	40	10	0.8	15.1	3.9×10^{-3}	438.74	1

$$\begin{aligned} \frac{\epsilon_0 \epsilon_{r,low_frequency}}{K_{cell}} &= \frac{N}{4} \cdot LWC_0 \\ \Rightarrow C_0 &= \frac{4\epsilon_0 \epsilon_{r,low_frequency}}{NLWK_{cell}} \end{aligned} \quad (3.2)$$

From equation (3.2), we can see that the capacitance per unit area C_0 depends not only on the electric properties of medium (relative permittivity at low frequency), but also sensor’s geometric.

The blood has a relative permittivity around 5300 at low frequency and approximately 60 at the high frequency [14, 17]. Therefore, we can determine the capacitance per unit area, depending on the structure of the sensor and medium.

Finally we estimate the parameters at the double layer DL (relative permittivity $\epsilon_{r,DL}$ and thickness d_{DL}) from equation (3.2). Fig. 10 presents the parameters of double layer. Table 1 indicates the results calculated the capacitance per unit area C_0 and the parameters of double layer.

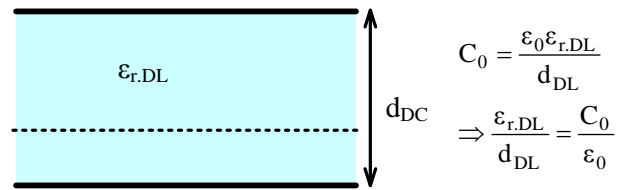


Fig. 10 – Parameters of double layer

4. RESULTS AND DISCUSSION

The main objective of this simulation is the verification of the analytical results from the theoretical development of equations relating the geometric parameters of the sensor and cut-off frequencies. We also study the influence of the metallization ratio on the impedance spectroscopy (IS).

A sinusoidal signal (1 volt) applied between terminals of interdigitated electrodes and a frequency range from 10 Hz to 1 GHz. We used the Manhattan mesh for this physical model, with linear elements sized 10 μm in the three directions (X, Y, Z). The model is presented in Fig. 11.

The electrical impedance Z is defined from the equation (2.6) by the data capacitance C and susceptance G (which are given by the CoventorWare software). As shown in Fig. 12, we present the simulation results of the impedance as function of frequency for several sensor types ($a = 0.3$; $a = 0.6$ and $a = 0.8$). The obtained results which presented in Fig. 12 and Table 2 demonstrate that the sensor type two “optimized” has the lowest cut-off frequency.

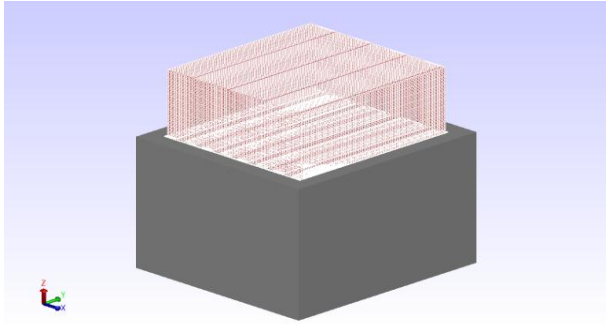


Fig. 11 – The schematic of sensor and Manhattan mesh model

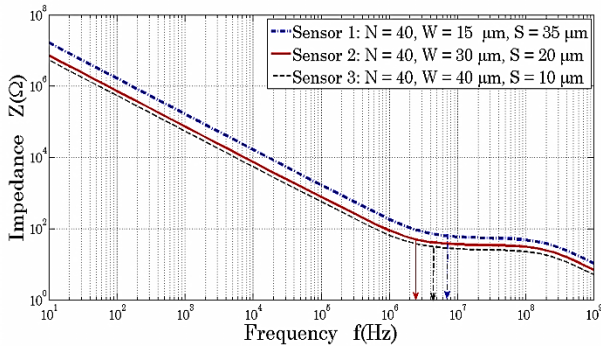


Fig. 12 – The relative between the electrical impedance and frequency range (Hz) for three different sensors

Table 2 – The geometric parameters of the sensor and cut-off frequencies of sensors

Sensor	L (mm)	N	W (μm)	S (μm)	α	f _{cut-off} (Hz)
1	2	40	15	35	0.3	7 × 10 ⁶
2	2	40	30	20	0.6	2.5 × 10 ⁶
3	2	40	40	10	0.8	4 × 10 ⁶

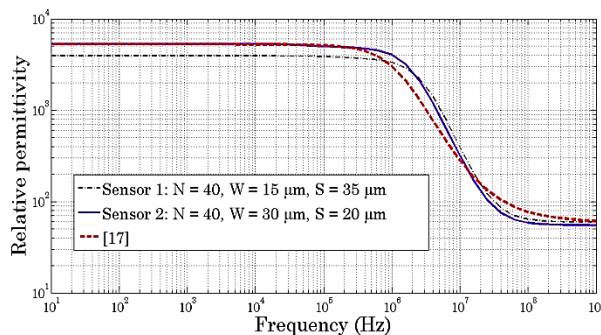


Fig. 13 – Relative permittivity as a function of the frequency

The relative permittivity ϵ of the medium is calculated from the data C obtained by the Coventor software and formula (2.5). Fig. 13 shows the relative per-

mittivity as a function of the frequency. In this figure, the curve of the relative permittivity of sensor two ($N = 40, W = 15 \mu\text{m}, S = 35 \mu\text{m}, L = 2 \text{mm}$) is more coincide with the curve from [17]. The result of blood's relative permittivity is approximately equal to 5300 at low frequency and 55 at the high frequency. It justifies that the optimization theory is correct.

5. CONCLUSION

This paper presents a physical model of interdigitated sensor in the frequency range 10 Hz-1 GHz. A theoretical approach is proposed to optimize the use of the sensor for bio impedance spectroscopy.

The results of analytical and numerical simulation demonstrate the advantage of the optimization to extend the usable bandwidth frequency of the sensor. By analyzing the equivalent circuit model we conclude that the capacitance per unit area depends on the medium electrical properties and sensor's geometric parameter.

The determination of capacity per unit area permits us to achieve the parameters of double layer. The simulation results present that the criteria which used to optimize of sensor are correct.

Finally, this paper presents a comparative approach for simulation of biological sensor modeling using CoventorWare software. Three dimensional interdigital sensor simulation techniques were done to analyze the influence of the physical properties of the medium and the impedance response by optimizing the geometry of sensor.

APPENDIX

The polarization appears at the contact surface between the electrodes and the solutions, it is an error cause in the measurement process.

The polarization impedance may be determined by the following expression:

$$Z_p = \frac{1}{j\omega C_{\text{interface}}}$$

In the reason to reduce the influence of polarization in the measurement, interdigital sensors must remain the maximum capacitance value interface.

By replacing C_0 from equation (3.2), the equation (2.4) becomes:

$$C_{\text{interface}} = \frac{\epsilon_0 \cdot \epsilon_{\text{low-frequency}}}{K_{\text{cell}}}$$

From this formula, we can conclude that the sensor which has smaller cell factor K_{cell} , it will be reduced the maximum polarization. Thus, the optimization of the cell factor K_{cell} is necessary.

REFERENCES

1. B. Pejčić, R. De Marco, *Electrochim. Acta* **51**, 6217 (2006).
2. R. Igreja, C.J. Dias, *Sens. Actuat. A: Phys.* **112**, 291 (2004).
3. C.R. Bowen, L.J. Nelson, R. Stevens, M.G. Cain, M. Stewart, *J. Electroceramics* **16** No4, 263 (2006).
4. F. Alexander, D.T. Price, S. Bhansali, *J. Phys. Conf. Ser.* **224**, 012134 (2010).
5. L. Wang, H. Wang, K. Mitchelson, Z. Yu, J. Cheng, *Biosens. Bioelectron.* **24**, 14 (2008).

6. M. Ibrahim, J. Claudel, D. Kourtiche, B. Assouar, M. Nadi, *New Developments and Applications in Sensing Technology* **83**, 169 (2011).
7. M. Ibrahim, J. Claudel, D. Kourtiche, M. Nadi, *J. Electr. Bioimpedance* **4**, 13 (2013).
8. F. Starzyk, *Archiv. Mater. Sci. Eng.* **34** No1, 31 (2008).
9. N.J. Kidner, Z.J. Homrighaus, T.O. Mason, E.J. Garboczi, *Thin Solid Films* **496**, 539 (2006).
10. C. Jungreuthmayer, G.M. Birnbaumer, P. Ertl, J. Zanghellini, *Sensor. Actuat. B: Chem.* **162**, 418 (2012).
11. W. Olthuis, W. Streekstra, P. Bergveld, *Sensor. Actuat. B: Chem.* vol. **24**, 252 (1995).
12. B. Timmer, W. Sparreboom, W. Olthuis, P. Bergveld, A. van den Berg, *Lab Chip*, **2** No2, 121 (2002).
13. Juan Prado Olivarez, *Conception et réalisation d ' un microsystème de mesure par spectroscopie de bioimpédance*, Thèse de l'Université Henri Poincaré - Nancy 1, (2006).
14. Laurent Bernard, *Caractérisation électrique des tissus biologiques et calcul des phénomènes induits dans le corps humain par des champs électromagnétiques de fréquence inférieure au GHz*, Thèse de l'Ecole Centrale de Lyon, (2007).
15. Jean-François Chateaux, *Conception et réalisation d'une cellule de caractérisation des tissus biologiques par spectroscopie de bioimpédance dans la gamme fréquentielle [100 Hz – 1 MHz]. Application aux tissus osseux – Prise en compte de l'anisotropie*, Thèse de l'Université Henri Poincaré, Nancy I, (2000).
16. S. Microtechnique, *Two-dimensional microimpedance imaging for cell culture monitoring* **3604**, (2006).
17. Ifac 2012, *Calculation of the Dielectric Properties of Body Tissues in the frequency range 10Hz-100GHz*. [Online].